ADVANCED FUNCTIONAL MATERIALS
www.afm-journal.de

Carbon Nanotube Fiber Based Stretchable Conductor

*Mei Zu, Qingwen Li, Guojian Wang, Joon-Hyung Byun, and Tsu-Wei Chou**

Carbon nanotube (CNT) based continuous fiber, a CNT assembly that could potentially retain the superb properties of individual CNTs on a macroscopic scale, belongs to a fascinating new class of electronic materials with potential applications in electronics, sensing, and conducting wires. Here, the fabrication of CNT fiber based stretchable conductors by a simple prestraining-then-buckling approach is reported. To enhance the interfacial bonding between the fibers and the poly(dimethylsiloxane) (PDMS) substrate and thus facilitate the buckling formation, CNT fibers are first coated with a thin layer of liquid PDMS before being transferred to the prestrained substrate. The CNT fibers are deformed into massive buckles, resulting from the compressive force generated upon releasing the fiber/substrate assembly from prestrain. This buckling shape is quite different from the sinusoidal shape observed previously in otherwise analogous systems. Similar experiments performed on carbon fiber/PDMS composite film, on the other hand, result in extensive fiber fracture due to the higher fiber flexural modulus. Furthermore, the CNT fiber/PDMS composite film shows very little variation in resistance (≈1%) under multiple stretching-and-releasing cycles up to a prestrain level of 40%, indicating the outstanding stability and repeatability in performance as stretchable conductors.

1. Introduction

Flexible electronics which are stretchable, bendable, twistable and foldable provide users with multifunctions and open up many new applications, ranging from stretchable displays[1] and photovoltaic devices[2] to skin sensors[3] and electronic eyeball cameras.[4] In recent years, a popular strategy to fabricate stretchable conductors is to form wavy or buckled structures by releasing a prestrained elastomeric substrate with an upper layer of conductive materials,[5,6] such as silicon films,[7] silicon nanowires[8] and carbon nanotubes (CNTs).[9] The basic principle of this method is remarkably straightforward and the fabricated wavy or buckled structures can accommodate applied strains by simply increasing the buckling wavelength and decreasing the buckling amplitude, without inducing significant strains in the flexible structures.

CNTs, which possess high mechanical performance and excellent electrical conductivity, have emerged as a potential material for stretchable conductors.[10] So far, CNT assemblies at various hierarchical structural levels have been utilized to fabricate CNT-based flexible conductors. At the 3D level, single-walled CNTs (SWNTs) and ionic liquid were dispersed in a fluorinated copolymer matrix to prepare rubber-like conductive composites which demonstrated high conductivity and excellent stretchability.[11] However, this rubber-like composite showed deteriorated conductivity when stretched and its fabrication process was complicated. At the 2D level, CNT films consisting of randomly oriented CNTs and well aligned CNT ribbons drawn from vertically grown CNT arrays were placed on top of or embedded in poly(dimethylsiloxane) (PDMS) to fabricate stretchable conductors.[12–16] However, stable electrical resistances of these stretchable conductors were accomplished only after several stretching-and-releasing cycles.

CNT-based continuous fiber, a CNT assembly that could potentially retain the superb properties of individual CNTs on a macroscopic scale at the 1D level, has attracted considerable research interest.[17–19] CNT fibers can be fabricated by spinning continuously from CNT solutions,[20] CNT aerogels,[21] and CNT arrays.[22] Owing to their highly compacted 1D structures, CNT fibers are a fascinating new class of electronic materials with potential applications in electronics, sensing, and conducting wires.[23] In this paper, we report the fabrication of stretchable conductors based on buckled CNT fibers by a simple prestraining-then-buckling approach. Before being transferred to the prestrained substrate, CNT fibers were coated with a thin layer of liquid PDMS by a dip-coating method to enhance interfacial bonding between the fibers and the PDMS substrate and thus, facilitate the buckling formation. Upon curing and releasing of the prestrain, the CNT fibers

M. Zu, Prof. G. J. Wang
School of Materials Science and Engineering
Tongji University
4800 Cao'an Highway, Shanghai 201804, China
M. Zu, Prof. T.-W. Chou
Department of Mechanical Engineering and Center for Composite Materials
University of Delaware
130 Academy Street, Newark, DE 19716, USA
E-mail: chou@udel.edu
Prof. Q. W. Li
Suzhou Institute of Nano-Tech and Nano-Bionics
398 Ruoshui Road, Suzhou 215123, China
Dr. J.-H. Byun
Composites Research Center
Korean Institute of Materials Science
797 Changwon Daero, Changwon 641831, South Korea

DOI: 10.1002/adfm.201202174

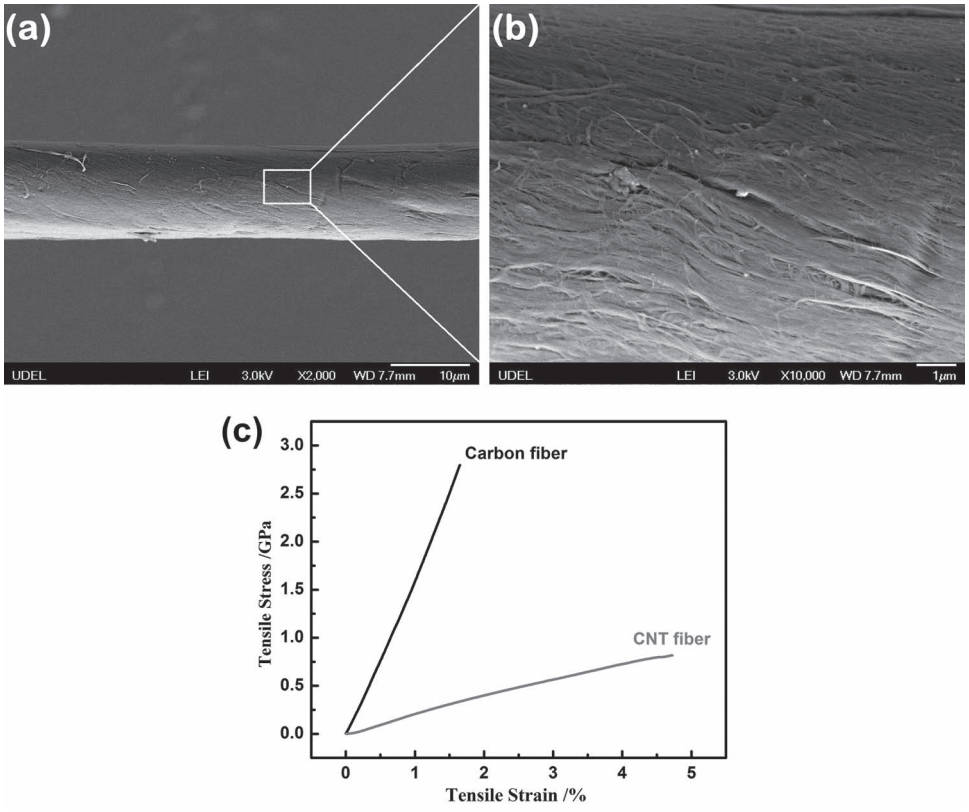

Figure 1. a) Surface mophorpogy of a CNT fiber under SEM. b) An enlarged view of the marked area in (a). c) Typical tensile stress-strain curves of a CNT fiber and a carbon fiber.

were kinked laterally. By contrast, the T300 carbon fibers adhered to the prestrained substrate were fractured into segments instead after release of the prestrain due to their high flexural modulus. A stretchable conductor was constructed by further coating the buckled CNT fibers with a thin layer of PDMS. The electrical resistance of the CNT fiber/PDMS composite film varied little (≈1%) under multiple cyclic tests up to a prestrain level of 40%.

2. Results and Discussion

The CNT fibers used in this study were spun by drawing and twisting CNT strips out of a vertically aligned array of CNTs, which were mainly double- and triple-walled with diameters of ≈6 nm.[24] **Figure 1**a shows the surface morphology of a CNT fiber observed by scanning electron microscopy (SEM, JSM-7400F). It can be seen that the fiber had a uniform diameter of around 13 μm. As shown in an enlarged view (Figure 1b), CNT bundles were tightly compacted due to ethanol infiltration during the spinning process. A typical CNT fiber tensile stress-strain curve is shown in Figure 1c. For comparison, T-300 carbon fiber specimens with diameters of 7 μm were also tested; the carbon fiber was much stronger and stiffer than the CNT fiber, whereas the latter had much higher strain to failure. Single CNT fiber tensile tests performed on 10 specimens gave a tensile strength of 0.82 ± 0.06 GPa, Young's modulus of 21.0 ± 1.8 GPa and strain to failure of 4.65 ± 0.20%.

Unlike well aligned CNT ribbons and randomly oriented CNT films, continuous fibers composed of pure CNTs do not form strong interfacial bonding with the PDMS substrate because of the much smaller total interfacial contact area. Thus, it is difficult for CNT fibers to spontaneously buckle in a periodic, wavy pattern as achieved in analogous systems of silicon nanoribbons and nanowires,[7,8] CNT ribbons and films.[12–15] Therefore, in order to facilitate fiber buckling, it is necessary to use an adhesive to enhance the bonding between the fibers and the substrate. In this study, liquid PDMS in an uncured state (a mixture of base and curing agent at a weight ratio of 10:1) was selected based on two considerations. First, the viscosity of the liquid PDMS at room temperature is high enough to adhere the fibers firmly to the substrate surface. Second, since the adhesive will be integrated into the PDMS substrate after curing, no "alien" substance is introduced to the whole device.

Figure 2 shows schematically the fabrication process of a flexible composite with buckled CNT fibers. For simplicity of the model system five CNT fibers, each 60 mm in length, were first laid parallel to one another with their ends fixed to two tape strips. The space between two adjacent fibers was kept at roughly 1.5 mm. Then, the aligned fibers were dipped into a degassed PDMS bath. It is worth noting that the liquid did not coat the fiber ends, which were used for electrode preparation. After dipping for 30 s at room temperature, the fibers coated with a thin layer of liquid PDMS were transferred to a prestretched PDMS substrate with a length of $L+\Delta L$. The whole

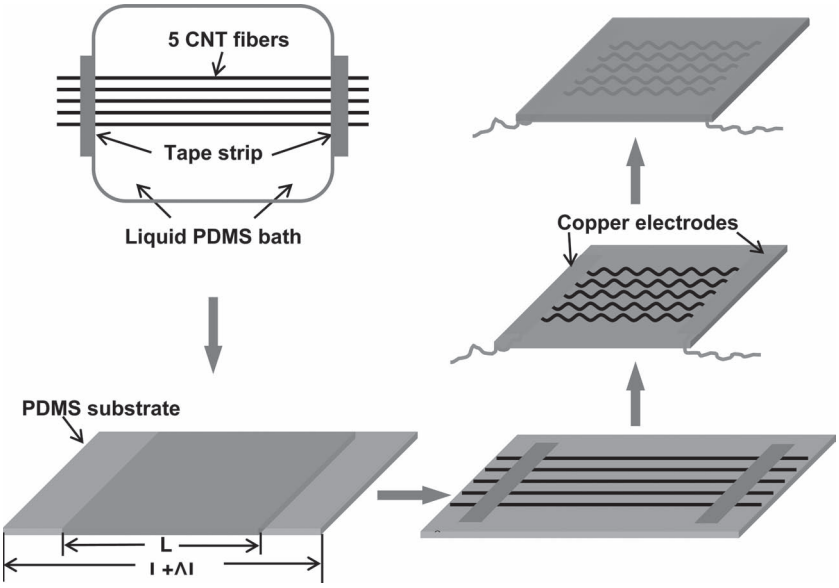

Figure 2. Illustration of the fabrication process of buckled CNT fibers sandwiched in between PDMS.

specimen was then cured in an oven at 100 °C for 1 h. After releasing the prestrain in the PDMS substrate, the fibers underwent compression and formed kinked patterns. Thin copper strips serving as electrodes were adhered to the two ends of kinked fibers by silver paint. Finally, a thin layer of uncured PDMS was cast on the top to enclose the device and the whole specimen was cured again in the oven at 100 °C for 1 h to in order to cure the top PDMS layer, resulting in CNT fibers sandwiched in between PDMS.

SEM images of one of the buckled CNT fibers under different magnifications are shown in **Figure 3**. Figure 3a shows massive buckles formed in the fiber, resulting from the compressive force generated upon releasing the fiber/substrate assembly from prestrain. This deformation in the form of kinking is a typical compressive failure mode of CNT fibers, which has been observed in our previous studies.[25,26] The excess PDMS present on the substrate above the buckled fiber appears as a result of the fiber dip-coating. During the transferring and aligning process, the fiber moved from the position where the excess PDMS is located to its present location, leaving a small amount of PDMS liquid at the initial contact position with the substrate. As can be seen from Figure 3b, the buckling shape of the CNT fiber is quite different from the sinusoidal shape observed in otherwise similar systems.[7–9,12–15] This is attributed to the discrepancy in their deformation mechanisms. Unlike the dense and continuous structure of other conductive materials (such as silicone nanowires and silicone ribbons) that can be elastically deformed upon stretching and releasing, the microstructure of the CNT fiber consists of a network of CNT bundles which are held by the weak van der Waals force. Therefore, slippage among these bundles could easily occur and this sliding is often believed as plastic deformation. When the fiber/substrate assembly was stretched back up to the prestrain level, the buckled fiber was straightened again, although the kink bands were still observed along the fiber. It should be noted that since there exist significant gap and void space between bundles of CNTs within the fiber, the liquid PDMS coating on the fiber could easily infiltrate into the inter-bundle void region. Therefore, the slippage among CNT bundles within the fiber and the extent of liquid infiltration needs to be fully examined in our future work for establishing a theoretical model to characterize the buckling mechanism of CNT fibers.

The lateral kinking pattern of the CNT fiber is further validated by a color 3D image of the kinked CNT fiber (Figure 3c) taken by a 3D laser scanning microscope (VK-X200, Keyence). It can be seen that the height of the kinked fiber was in the range of ≈20–30 μm, much higher than that of the fiber diameter which was around 13 μm. This increase in the height of the CNT fiber is probably due to the thickness of the PDMS layer coating on the fiber. As shown in the enlargement of two buckles in the fiber (Figure 3d), the CNT bundles on the compressive side of the fiber buckled without apparent damage to the fibers, resulting in the outward movement of the neutral plane, which effectively reduced the stress on the tensile side of the fiber, as also observed in aerogel-spun CNT fibers subject to bending.[27] Moreover, the buckled CNT fiber can be alternatively straightened and kinked without apparent permanent fracture under stretching-and-releasing cycles. This excellent stability and repeatability of the kinking of the CNT fibers are of critical importance in retaining the fiber electrical conductivity during cyclic loading, and therefore performance of CNT fiber based stretchable conductors.

Since the electrical conductivity of a single carbon fiber (6.34×10^4 S m^{-1}) is comparable to that of the current CNT fiber (4.75×10^4 S m^{-1}), a carbon fiber composite was also fabricated using the same procedure as that for the CNT fiber/PDMS film depicted in Figure 2. The prestrain level was also set at 40%. However, it was difficult to adhere the carbon fiber to the PDMS substrate by the dip-coating method. Upon releasing the prestrain of the substrate, the carbon fiber slid easily because of the poor interfacial bonding between the fiber and the substrate. Therefore, in order to enhance the interfacial bonding between the carbon fiber and the substrate, PDMS droplets were applied to the carbon fiber which had been already laid on the substrate. Figure 3e is an optical microscopy image of a carbon fiber after the release of prestrain. It can be seen that instead of deforming into a continuously buckled pattern, the carbon fiber was fractured into segments. Furthermore, a comparison of Figure 3b,e shows that the "wavelength" and "amplitude" of the kinked CNT fiber were much smaller than those of the carbon fiber. The SEM image of Figure 3f further demonstrates the brittle nature of carbon fiber fracture.

The divergence in the response to external compressive stress of the two kinds of fibers is attributed to the fact that the CNT fiber has a much lower flexural modulus than the carbon fiber. Because the microstructure of the CNT fiber consisted of a network of CNT bundles, it was feasible for it to bend in ways that the carbon fiber with a more dense structure cannot. This high

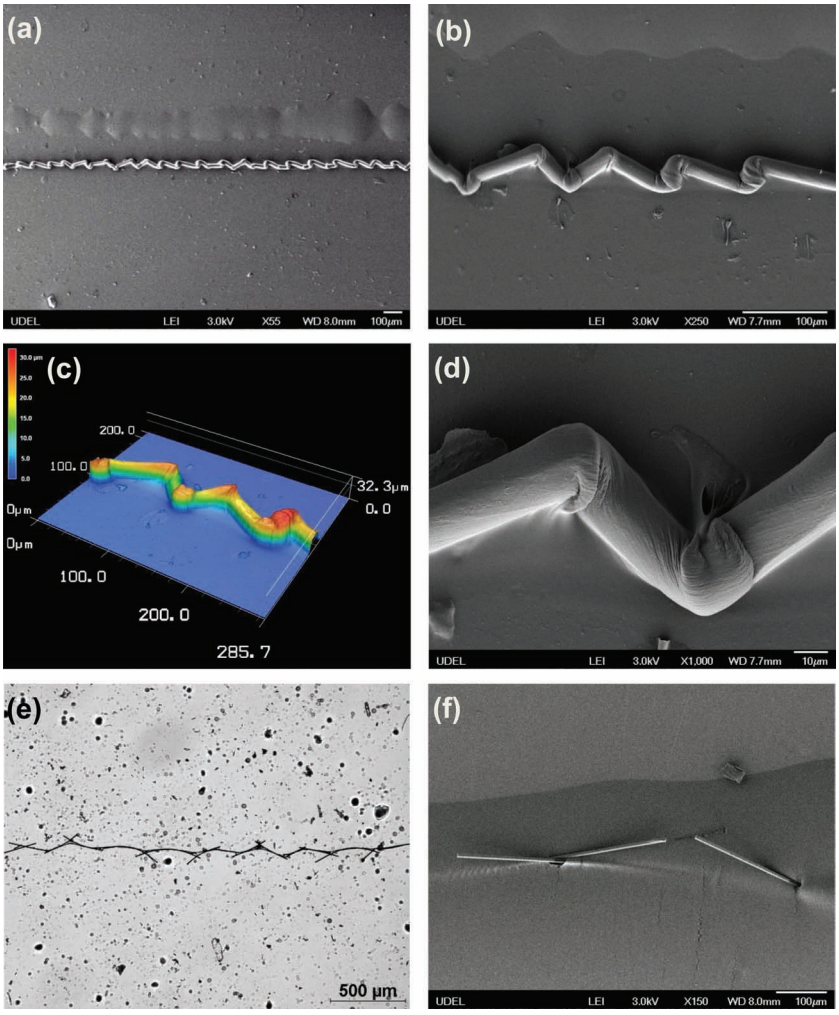

Figure 3. a,b) Low-magnification SEM images of one kinked CNT fiber. c) A color 3D image of the kinked CNT fiber taken by a laser microscope. d) An enlarged SEM view of two kinks in the CNT fiber. e) Optical microscopy image of one carbon fiber after releasing the prestrain of PDMS substrate. f) An enlarged SEM view of the fractured carbon fiber.

flexibility of CNT fibers was also reported by Vilatela et al.[27] In the present study, when the prestrain of the substrate was elevated to 100% and the interfacial bonding was enhanced by a thick layer of liquid PDMS instead of dip-coating, the resulting CNT fiber composite was still flexible enough to buckle into small "wavelength" and "amplitude" without fracture.

The high flexibility that CNT fibers demonstrated is an essential prerequisite of the fabrication of kinked CNT fiber-based stretchable conductors. A stretchable conductor with five kinked CNT fibers sandwiched in between PDMS is shown in **Figure 4**a. It can be seen that the kinked fibers remain aligned and look fairly "straight" to the naked eye. The performance of the CNT fiber/PDMS composite film as a stretchable conductor was tested on a microstraining frame under cyclic tensile loading, while its electrical resistance was measured in real time. It should be noted that the total resistance of the CNT fiber/PDMS composite film was determined by the amount of fibers laid on the substrate. The electrical resistance of single CNT fiber with a length of 60 mm was around 1.2×10^4 Ω. It was expected that the total electrical resistance of the composite film with five fibers arranged in a parallel configuration decreased to one fifth of the single fiber value, around 2.6×10^3 Ω. Figure 4b plots the measured resistance of the CNT fiber/PDMS film during cyclic stretching to the prestrain level of 40%. It can be seen that the resistance of the composite film increased slightly with increasing tensile strain by only about 30 Ω (1%) up to the prestrain level. Upon release, the resistance showed a corresponding decrease, eventually returning to its initial state. This trend of resistance variation was maintained in multiple stretching-and-releasing cycles up to the prestrain level (Figure 4b). This observation is due to the fact that the conductivity of the CNT fibers is dictated by the conductivity of the individual CNTs as well as the degree of electrical contact established between individual CNTs.[18] Even though sliding did occur among CNT bundles upon stretching and releasing, there was no slippage occurring between the fibers and the substrate due to the strong interfacial bonding that was enhanced by the liquid PDMS after cure. Therefore, the total intertube contact area within the fiber was kept nearly constant and hence, a stable electrical resistance of the composite film could be expected. It should be noted that the fiber tensile failure strain is around 5%, which is much less than that of the CNT web (or film).[28] Therefore, the kinked CNT fibers are stretchable before straightening and their stretchability depends largely on the applied prestrain.

3. Conclusions

We have fabricated CNT fiber based stretchable conductors by a simple prestraining-then-buckling approach. To enhance the interfacial bonding between the fibers and the PDMS substrate and thus facilitate the buckling formation, CNT fibers were first coated with a thin layer of liquid PDMS before being transferred to the prestrained substrate. Upon release of the prestrain, the CNT fibers were readily kinked in-plane because of their high flexibility. Similar experiments performed on a carbon fiber/PDMS composite film, on the other hand, resulted in extensive fiber fracture due to the higher fiber flexural modulus. Furthermore, the CNT fiber/PDMS composite film showed very little variation in resistance (≈1%) under multiple stretching-and-releasing cycles up to a prestrain level of 40%, indicating the outstanding stability and repeatability in performance as stretchable conductors. Together with their continuously improving mechanical performance, CNT fibers possessing the unique stretchability demonstrated in the present study are expected to

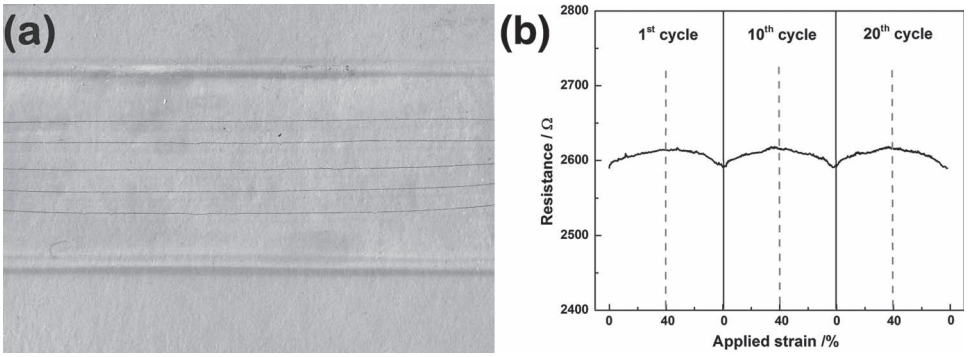

Figure 4. a) Photograph of a stretchable conductor with five kinked CNT fibers sandwiched in between PDMS films. b) Electrical resistance of a CNT fiber/PDMS composite film during cyclic stretching to the prestrain level of 40%. Only the data of the 1st, 10th, and 20th cycles are shown for comparison.

further improve their applicability as reinforcements for multifunctional composites.

4. Experimental Section

Preparation of PDMS Substrate: The PDMS substrate was prepared by mixing a silicone-elastomer base and curing agent (Sylgard 184, Dow Corning) at a ratio of 10:1 by weight. The mixture was first degassed under vacuum then poured onto a glass substrate, followed by curing at 100 °C for 1 h. The thickness of the resulting film was in the range of ≈0.4–0.5 mm. A rectangular slab of 13 mm × 80 mm was cut from the polymerized piece.

Electrical Characterization: The CNT fiber/PDMS composite films were repeatedly stretched and released by a microstraining frame, while their electrical resistance was measured in real time by a four-point method utilizing a Keithley 2182A Nanovoltmeter in conjunction with a Keithley 6430 Sub Femtoamp Remote Sourcemeter.

Acknowledgements

This work was partially supported by the US Air Force Office of Scientific Research (Dr. Byung-Lip Lee, Program Director), the National Research Foundation of Korea (NRF) through a grant provided by the Korean Ministry of Education, Science and Technology (MEST) and the Office of Naval Research (Dr. Yapa Rajapakse, Program Director). The authors thank Dr. Weibang Lu and Dr. Amanda Wu for helpful discussions. Prof. Bingqing Wei's advice on specimen preparation is also appreciated. M.Z.'s study abroad at the University of Delaware is supported by the State Scholarship Fund of the China Scholarship Council.

Received: August 1, 2012
Published online: September 18, 2012

[1] G. H. Gelinck, H. E. A. Huitema, E. van Veenendaal, E. Cantatore, L. Schrijnemakers, J. B. P. H. van der Putten, T. C. T. Geuns, M. Beenhakkers, J. B. Giesbers, B.-H. Huisman, E. J. Meijer, E. M. Benito, F. J. Touwslager, A. W. Marsman, B. J. E. van Rens, D. M. de Leeuw, *Nat. Mater.* **2004**, *3*, 106.
[2] Y. Sun, W. M. Choi, H. Jiang, Y. Y. Huang, J. A. Rogers, *Nat. Nanotechnol.* **2006**, *1*, 201.
[3] T. Someya, Y. Kato, T. Sekitani, S. Iba, Y. Noguchi, Y. Murase, H. Kawaguchi, T. Sakurai, *Proc. Natl. Acad. Sci. USA* **2005**, *102*, 12321.
[4] H. C. Ko, M. P. Stoykovich, J. Song, V. Malyarchuk, W. M. Choi, C.-J. Yu, J. B. Geddes III, J. Xiao, S. Wang, Y. Huang, J. A. Rogers, *Nature* **2008**, *454*, 748.
[5] N. Bowden, S. Brittain, A. G. Evans, J. W. Hutchinson, G. M. Whitesides, *Nature* **1998**, *393*, 146.
[6] D.-H. Kim, J. A. Rogers, *Adv. Mater.* **2008**, *20*, 4887.
[7] D.-Y. Khang, H. Jiang, Y. Huang, J. A. Rogers, *Science* **2006**, *311*, 208.
[8] S. Y. Ryu, J. Xiao, W. I. Park, K. S. Son, Y. Y. Huang, U. Paik, J. A. Rogers, *Nano. Lett.* **2009**, *9*, 3214.
[9] D.-Y. Khang, J. Xiao, C. Kocabas, S. MacLaren, T. Banks, H. Jiang, Y. Y. Huang, J. A. Rogers, *Nano. Lett.* **2007**, *8*, 124.
[10] J. A. Rogers, T. Someya, Y. Huang, *Science* **2010**, *327*, 1603.
[11] T. Sekitani, Y. Noguchi, K. Hata, T. Fukushima, T. Aida, T. Someya, *Science* **2008**, *321*, 1468.
[12] Y. Zhu, F. Xu, *Adv. Mater.* **2012**, *24*, 1073.
[13] F. Xu, X. Wang, Y. Zhu, Y. Zhu, *Adv. Funct. Mater.* **2012**, *22*, 1279.
[14] Y. Zhang, C. J. Sheehan, J. Zhai, G. Zou, H. Luo, J. Xiong, Y. T. Zhu, Q. X. Jia, *Adv. Mater.* **2010**, *22*, 3027.
[15] C. Yu, C. Masarapu, J. Rong, B. Wei, H. Jiang, *Adv. Mater.* **2009**, *21*, 4793.
[16] K. Liu, Y. H. Sun, P. Liu, X. Y. Lin, S. S. Fan, K. L. Jiang, *Adv. Funct. Mater.* **2011**, *21*, 2721.
[17] T. W. Chou, L. M. Gao, E. T. Thostenson, Z. G. Zhang, J. H. Byun, *Compos. Sci. Technol.* **2010**, *70*, 1.
[18] W. Lu, M. Zu, J.-H. Byun, B.-S. Kim, T.-W. Chou, *Adv. Mater.* **2012**, *24*, 1805.
[19] A. S. Wu, T. W. Chou, *Mater. Today* **2012**, *15*, 302.
[20] B. Vigolo, A. Penicaud, C. Coulon, C. Sauder, R. Pailler, C. Journet, P. Bernier, P. Poulin, *Science* **2000**, *290*, 1331.
[21] Y. L. Li, I. A. Kinloch, A. H. Windle, *Science* **2004**, *304*, 276.
[22] Q. W. Li, X. F. Zhang, R. F. DePaula, L. X. Zheng, Y. H. Zhao, L. Stan, T. G. Holesinger, P. N. Arendt, D. E. Peterson, Y. T. Zhu, *Adv. Mater.* **2006**, *18*, 3160.
[23] Q. W. Li, Y. Li, X. F. Zhang, S. B. Chikkannanavar, Y. H. Zhao, A. M. Dangelewicz, L. X. Zheng, S. K. Doorn, Q. X. Jia, D. E. Peterson, P. N. Arendt, Y. T. Zhu, *Adv. Mater.* **2007**, *19*, 3358.
[24] J. J. Jia, J. N. Zhao, G. Xu, J. T. Di, Z. Z. Yong, Y. Y. Tao, C. O. Fang, Z. G. Zhang, X. H. Zhang, L. X. Zheng, Q. W. Li, *Carbon* **2011**, *49*, 1333.
[25] A. S. Wu, T. W. Chou, J. W. Gillespie Jr., D. Lashmore, J. Rioux, *J. Mater. Chem.* **2012**, *22*, 6792.
[26] M. Zu, W. Lu, Q. W. Li, Y. Zhu, G. Wang, T. W. Chou, *ACS Nano* **2012**, *6*, 4288.
[27] J. J. Vilatela, A. H. Windle, *Adv. Mater.* **2010**, *22*, 4959.
[28] W. J. Ma, L. Q. Liu, R. Yang, T. H. Zhang, Z. Zhang, L. Song, Y. Ren, J. Shen, Z. Q. Niu, W. Y. Zhou, S. S. Xie, *Adv. Mater.* **2009**, *21*, 603.